Surface plasmon resonance effects of gold colloids on optical properties of N719 dye in ethanol

MOHAMMED A. AL-AZAWI[a], N. BIDIN[b*], M. ABDULLAH[b], ABDULRAHMAN K. ALI[c], KHALEEL I. HASSOON[c], N. A. KHALDOON[a], HAYDER J. Al-ASEDY[a]
[a]*Universiti Teknologi Malaysia, Faculty of Science, Department of Physics, Johor Bahru, Johor, Malaysia, 81310*
[b]*Universiti Teknologi Malaysia, Ibnu Sina Institute for Scientific and Industrial Research, Laser Center, Johor Bahru, Johor Malaysia, 81310*
[c]*University of Technology, Department of Applied Sciences, Laser and Optoelectronics Branch, Baghdad, Republic of Iraq, 10066*

In this work, the light absorption and emission effects of gold nanoparticles on some optical properties of N719 dye solution were studied via transmission electron microscopy, UV-vis absorption, and photoluminescence spectroscopy measurements. A facile method to fabricate four gold colloidal solutions with different concentrations containing ~15 nm gold nanoparticles was presented through pulsed laser ablation of a gold target immersed in ethanol, followed by a post-ablated size modification process. As-prepared gold colloids with different concentrations were mixed with certain dye solution. The absorption and fluorescence enhancement that resulted from the interaction between the dipole moments of the day and the surface plasmon resonance of gold nanoparticles were found to be strongly dependent on the gold colloid concentration. Fluorescence was enhanced by around 9-fold, which was achieved for the dye solution with the highest gold nanoparticles concentration.

(Received February 13, 2015; accepted March 19, 2015)

Keywords: Gold nanoparticles; Surface plasmon resonance; Fluorescence; N719 dye

1. Introduction

Noble metal nanoparticles such as gold nanoparticles (AuNPs) are used as functional materials because of the collective oscillation of the conduction electrons of these materials, which is also known as localized surface plasmon resonance (LSPR) [1, 2]. The sharp-absorption peak of the LSPR of AuNPs at the visible region is important in modern innovations [3-5]. The interaction of surface plasmons in metal nanoparticles with the electric field of incident light can significantly change the plasmonic mode density localized in the vicinity of metal nanoparticles (i.e., localized near-electric fields) [6-8]. Enhanced light absorption of molecules adsorbed on metal nanoparticles is one of the most interesting features of LSPR behavior [9]. LSPR bands of AuNPs are located in the visible range of the electromagnetic spectrum. Currently intensive studies have been focused to tune and match LSPR bands of AuNPs with the absorption and emission bands of standard dyes. Such work has many technological applications including, dye-sensitized solar cells (DSSCs) [10-12], biological sensing applications [13, 14], and photocatalysts [15-17].

Furthermore, the optical cross-section of gold nanoparticles (10–50 nm in diameter) offers a fivefold absorption or more in magnitude than those of conventional dyes [18]. The energy attenuation of electromagnetic waves (i.e., total light extinction) after passing through a particulate medium results from two contributions: absorption and scattering. The extinction cross section σext of a single particle is expressed by [19,20]:

$$\sigma_{ext} = \sigma_{abs} + \sigma_{sca} \quad (1)$$

where σ_{abs} and σsca are the absorption and scattering cross-sections of a particle, respectively. LSPR frequencies strongly depend on the extinction cross-section of particles, which in turn depend on several parameters, such as the particle material, particle size and shape, surrounding medium, and number of particles [21-23]. The performance of nanoparticles is found to depend on a careful choice of these parameters.

Scattering and absorption are competing processes that can be predicted based on the optical properties of a material. A strong scattering and absorption of incoming light occurs when the frequency of light matches the natural frequency of LSPR in metal nanoparticles [24]. Moreover, the enhancement and quenching of the photoluminescence (PL) spectra are attributed to the scattering and absorption processes, respectively. The emission is quenched because absorption dominates scattering; by contrast, emission enhancement emanates from scattering dominating over absorption. Generally, scattering that results from metal nanoparticles is favored in light trapping applications, such as silicon solar cells [21, 25], while enhancing light absorption via metal nanoparticles has been utilized to improve most DSSC devices [26, 27]. Furthermore, strong quenching from the AuNPs effects is used to improve the efficiency of fluorescence sensor systems [28, 29]. Quenching indicates

decreasing the fluorescence intensity and can occur through different processes, such as collision, nonfluorescent complex formation, fluorescence resonance energy transfer (FRET), and a trivial process [30]. FRET is predominately an important process that describes the nonradiative energy transfer between a fluorephore (donor) and a quencher (acceptor) based on dipole–dipole coupling in the excited state through an electric field [31]. Metal nanoparticles can be used as donors or acceptors depending on the enhancement or quenching of emission, respectively.

Despite the popularity of using dye molecules, a relatively modest amount of work has been devoted to enhance light absorption and improve FRET mechanism in dye systems. In this work, we have studied the LSPR effects on optical absorption and fluorescence of N719 dye solutions in the presence and absence of AuNPs. Hence, different concentrations of AuNPs are synthesized through pulsed laser ablation of a gold target in ethanol. This technique allows the easy preparation of uncontaminated size-controlled nanoparticles [32-34]. When all the other parameters remain fixed during the experiment, the optical properties of the dye solution in the presence of AuNPs (i.e., dye@AuNPs solution) strongly depend on the concentrations of AuNPs.

2. Experimental setup

2.1 Synthesis of gold nanoparticles

A highly pure Au plate (purity, >99.999%) with a thickness of 2 mm and a diameter of 20 mm was employed in this research as a target material. After cleaning the Au plate ultrasonically in ethanol, the target was rinsed with deionized water to eliminate the contaminants. Subsequently, this target was maintained at the bottom of a pyrex vessel (volume, 15 mL) filled with 70 vol% ethanol (i.e., C_2H_6O:H_2O volume ratio). A pulsed Nd:YAG laser (fundamental wavelength, 1064 nm; pulse duration, 8 ns; repetition rate, 10 Hz) was employed as the irradiation source during the ablation. The experiments were conducted by operating the laser fluence at 20 J/cm^2 and focusing the beam on the target surface by using a converging lens with a 10 cm focal length at different ablation times. The ablation times were varied in the range of 4, 8, 15, and 20 min. Four Au colloidal solutions were produced with different concentrations, of 8×10^{11}, 1.6×10^{12}, 4.2×10^{12}, and 9×10^{12} particles/mL. During ablation, the Au colloidal solution was continuously stirred using a magnetic stirring device at room temperature to disperse the produced AuNPs and to remove these particles from the laser path.

Once the ablated process was stopped, the Au target was removed from the ablated vessel. Post-ablated modification process was immediately performed by irradiating the colloidal solution with 1,064 nm laser pulses for 5 min. Each laser ablation and post-ablated size modification process generated almost similar nanoparticle sizes (~15 nm) in all Au colloidal solutions, which then labeled as S1, S2, S3, and S4.

2.2 Synthesis of N719 dye

A sensitizer, $[RuL_2(NCS)_2]$: 2TBA (L = 2,2'-bipyridyl-4,4'-dicarboxylic acid; TBA = tetra-n-butylammonium), which is also known as N719 dye (Fig. 1), was purchased from Dyesol. An extra pure (99.7%) 0.03 mM dye in ethanol was prepared and labeled as S0 solution. The optical properties of the dye solution with and without adding the different concentrations of AuNPs solution were investigated. The dye with AuNPs (i.e., dye@AuNPs) was prepared by adding 0.1 mL of as-prepared Au colloids to 1.5 mL of dye solution.

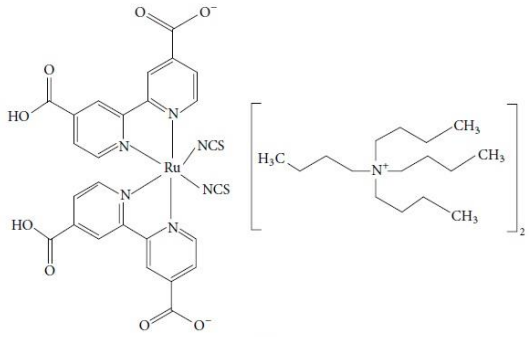

Fig. 1. Chemical structure of the N719 dye.

2.3 Instruments

The absorption spectra of all samples S0, S1, S2, S3, and S4 were characterized using a UV-vis spectrophotometer (Perkin-Elmer, Lambda 25) with a quartz cuvette (path length: 0.5 cm). The photoluminescence (PL) spectra of these samples were recorded using a spectrometer (Perkin-Elmer, Luminescence LS55) at an excitation wavelength of 350 nm with a quartz cuvette (path length: 1 cm). A transmission electron microscope (TEM; Philips CM12; accelerating voltage: 120 kV) was used to obtain the micrographs of AuNPs. Hence, the Au colloidal solution was placed in an ultrasonic bath for 20 min. Subsequently, a small drop of the sample solution was placed on a carbon-coated copper grid and then dried at room temperature. The average particle size and size distribution of each Au colloidal solution were determined by counting more than 250 particles in the TEM image by using the ImageJ software.

3. Results and discussion

Fig. 2 shows the typical UV-vis absorption spectra of the Au colloidal solutions. The solutions were produced through the 1,064 nm laser ablation of the Au target in ethanol at various ablation times (4, 8, 15, and 20 min) and the subsequent treatment via the laser-induced particle modification process by irradiating these solutions by using 1,064 nm laser pulses for 5 min. The post-ablated modification allowed the selection of Au colloidal

solutions with nearly similar average particle sizes. The absorbance of gold colloids demonstrated the characteristic features of LSPR. The LSPR peak at around 521 nm was attributed to surface plasmon transitions, which strongly depended on the size and shape of the AuNPs [35]. The prominent single peaks indicated that the obtained nanoparticles were nearly spherical in the colloidal solution. The AuNPs morphologies were also verified through the TEM results. The tail part of the absorption band toward the UV range was ascribed to the interband transitions of AuNPs. The absorption intensity caused by the interband transitions at 450 nm did not appreciably shift with the particle size, but this intensity was proportional to the concentration of Au particles (CAu, i.e., number of particles per unit volume) [36, 37]. These observations agreed well with our CAu experimental data, which were calculated through the following equation [38]:

$$C_{Au} = \frac{\Delta m}{\rho \times \frac{4}{3}\pi r^3 \times V} \quad (2)$$

where Δm is the mass loss of the target, which indicated the mass of the generated nanoparticles. The mass loss of the target was determined according to the weight of the target which measured before and after the ablation process using a highly sensitive analytical digital balance with 0.01 mg readability. The parameters $\rho, r,$ and V are the gold density (19.3 g/cm^3), radius of single AuNPs, and volume of the working liquid, respectively. From Equation (2), the AuNPs concentrations in the produced colloidal solutions of S1, S2, S3, and S4 were computed to be about 8×10^{11}, 1.6×10^{12}, 4.2×10^{12}, and 9×10^{12} particles/mL, respectively. The measurements showed that the concentrations of AuNPs depended on the ablation time. As the ablation time increased, the concentration is also increased, as shown in the inset of Figure 2. This finding indicates an increase in the plasmon intensity, which become the subject of study in this work.

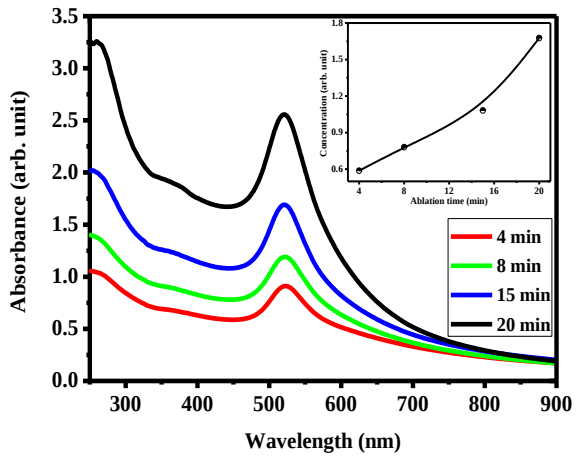

Fig 2. UV-vis absorption spectra of the Au colloidal solution prepared via laser ablation of a gold target in ethanol at various ablation times. The inset shows the produced AuNPs as a function of ablation time.

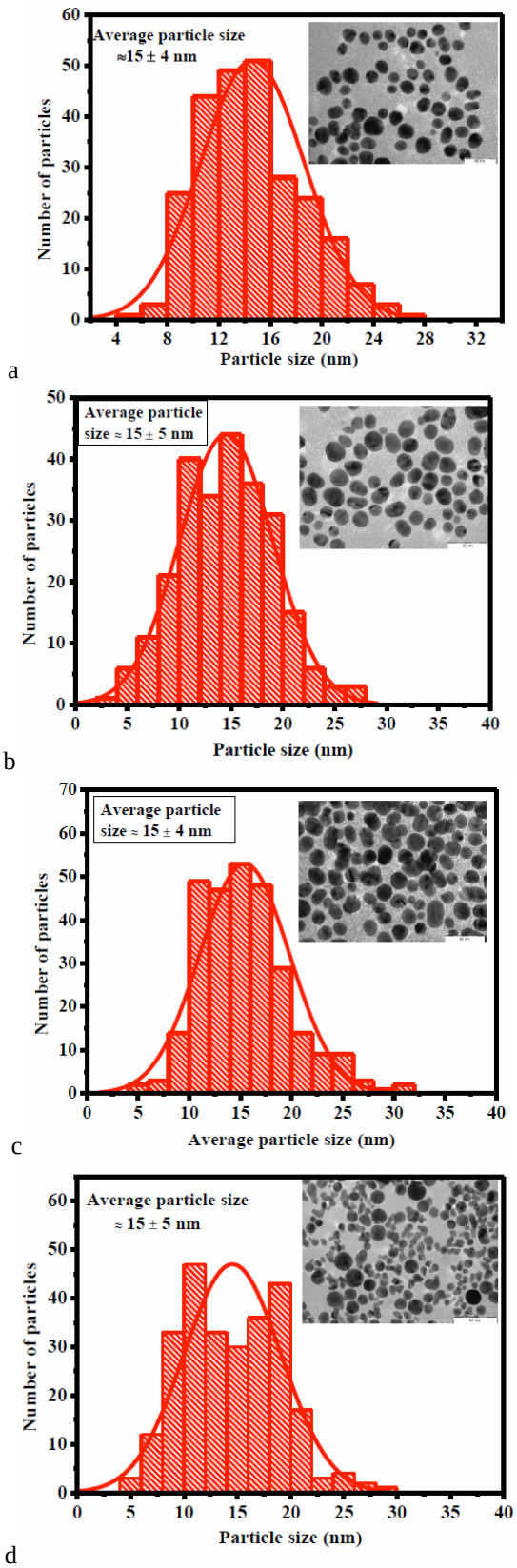

Fi.g 3. TEM micrograph and histogram (inset) of the gold nanoparticles: (a) S1, (b) S2, (c) S3, and (d) S4, produced via laser ablation of the gold target in ethanol at different ablation times of 4, 8, 15, and 20 min, followed by the size modification and redistribution process of AuNPs under laser-induction for 5 min for each ablated solution.

Fig. 3a–d show the TEM images of AuNPs prepared by the laser-ablated Au target and the consecutive irradiation of the Au colloidal solution during laser ablation and post-ablated size modification processes, respectively. Each TEM image was accompanied by the histogram of the particle size distribution. The TEM images indicated that majority of the nanoparticles were spherical, possessed high electron density, and had unapparent aggregation. Based on the histograms, the particle size distribution was narrow with an average particle size that was closed to ~15 nm and almost similar in all the prepared Au colloidal solutions.

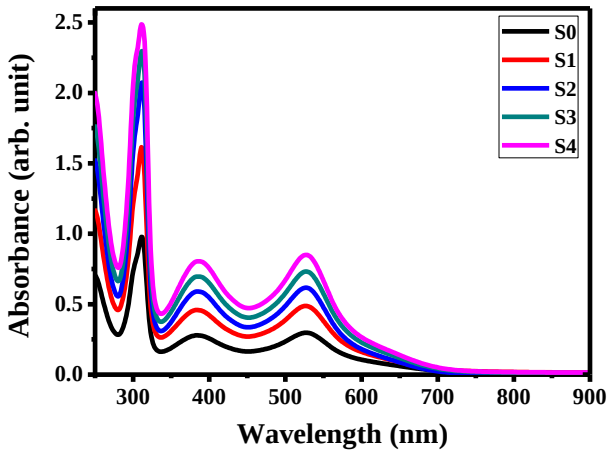

Fig. 4. UV-vis absorption spectra of the N719 dye solutions in the absence and presence of different concentrations of 0, 8 × 10^{11}, 1.6 ×10^{12}, 4.2 ×10^{12}, and 9 ×10^{12} particles/mL Au colloids for S0, S1, S2, S3, and S4, respectively.

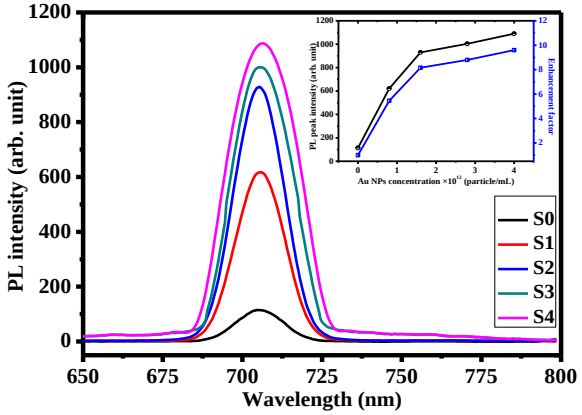

Fig 5. Photoluminescence spectra of the N719 dye solutions with and without different concentrations of 0, 8 × 10^{11}, 1.6 ×10^{12}, 4.2 ×10^{12}, and 9 ×10^{12} particles/mL Au colloids for S0, S1, S2, S3, and S4, respectively, under 350 nm excitation. The inset shows the variations in both PL peak intensity and enhancement factor with Au colloid concentrations.

The UV-vis absorption spectra of N719 dye solution with and/or without added various concentrations of Au colloids are described in Figure 4. The N719 dye molecules in ethanol had one absorption band of the UV region at around 311 nm and two other absorption bands of the visible region at 386 and 527 nm, respectively. The absorption band of the UV region was attributed to an electronic transition between the (π-π*) orbitals of the intra-ligand, whereas the bands of the visible region are caused by the metal-to-ligand charge transfer (MLCT) transitions [39, 40]. Generally, the MLCT band of the N719 dye solution at 527 nm became predominant in many applications. In dye-sensitized solar cells, the light absorption in the visible part of the solar spectrum was caused by an MLCT transition that generated electrons and holes [41]. Figures 2 and 4 show that the maximum relative enhancement of dye molecule absorption in the solution appeared at 527 nm and was close to the LSPR peak of Au colloids around 521 nm instead of the dye absorption peak at 386 nm, which suggested that the increase in dye absorption largely generated from the LSPR of AuNPs. The absorption peak of the dye@AuNP solution was found to increase as the concentration of Au colloids increases. The increment in dye molecule absorption could be attributed to an increase number of AuNPs. Thus increasing the total surface for surface plasmon resonance, which contributed to the increment in total absorption of the dye. Therefore, the interaction between the dye molecular dipole and the electric field of the incident light near the nanoparticle surface was augmented. The photoluminescence spectra from dye solutions in the absence and presence of AuNPs are shown in Figure 5. The photoluminescence emissions spectra of the prepared samples were measured at room temperature with a 350 nm excitation wavelength. An increase in the Au colloid concentration, the fluorescence intensities of the dye@AuNP solutions were significantly enhanced. The center of the PL band remained almost constant at 706 nm, and the spectra shape was unchanged in the presence of AuNPs. The PL enhancement factor was calculated through the ratio of the fluorescence intensity of the dye solution in the presence and absence of AuNPs, respectively. The dependence of both fluorescence intensity and enhancement factor on the concentration of AuNPs is shown in the inset of Figure 5. The inset exhibits the drastic increase in the enhancement factor and the fluorescence intensity of the dye@AuNP solution as the AuNPs concentration increases. The highest enhancement factor of the dye@AuNP solution at the AuNP concentration of the 9 ×10^{12} particles/mL was recorded to be 9-fold larger than the bare dye solution. The enhancement refers to the increase in the nonradiative energy transfer from AuNPs (donors) to the dye molecules (acceptors) by the FRET mechanism because of the increase in the interaction between the dye molecules and AuNPs. The enhancement also indicated that the increase in the AuNPs absorption of the incident light excited the dye molecules, which can exhibit the enhancement in fluorescence intensity. Moreover, the strongest fluorescence intensity of the dye@AuNPs solution

suggested that scattering was dominant over the absorption processes. These results verified that a certain interaction existed between the dipole moments of the dye and the LSPR of AuNPs that occurred, which meant that the dipole moments and the LSPR were within a minimal spatial range to transfer the resonance energy between the two [42, 43].

4. Conclusion

Each pulsed laser ablation technique of a gold bulk immersed in ethanol and the post-ablated size modification process were exploited to fabricate pure Au colloids at different concentrations. Nearly similar sizes of ~15 nm were selected for the prepared AuNPs. The TEM micrographs and UV-vis spectrophotometer results revealed that the synthesized AuNPs were pure spherical particles, homogenous, and possessed high electron density. These characteristics facilitated the use of AuNPs when studying some optical properties of dye solutions. The enhancement of the absorption and fluorescence of the dye@AuNP solution also occurred. This finding verified a certain interaction that existed between the dipole moments of the dye and the LSPR of AuNPs that occurred, which meant that these dipole moments and LSPR were within a minimal spatial range to transfer the resonance energy in between. At a constant size of AuNPs, an increase of Au colloid concentrations increased the total surface for surface plasmon resonance, which contributed to the increased total absorption by the dye. Moreover, the nonradiative energy was transferred by FRET mechanism from AuNPs to the dye molecules in the dye@AuNP solution after exciting the solution under the 350 nm PL excitation wavelength. Therefore, the absorbance and fluorescence intensities of dye@AuNPs were found to be increasingly with the Au colloid concentrations. Enhancement fluorescence was observed with the highest AuNPs concentration with a maximum enhancement factor of about 9-fold. The research results may offer a potential application of dye@AuNPs in the technological development of DSSC and other photonics fields.

Acknowledgment

We like to express our thanks to the government of Malaysia through FRGS vote 4F543 and UTM through RMC for the financial support of this project as well as monitoring the progress of the works.

References

[1] E. Hutter, J.H. Fendler. Advanced Materials. **16**, 1685 (2004).
[2] J. Lerme, C. Bonnet, M. Broyer, E. Cottancin, D. Manchon, M. Pellarin, Journal of Physical Chemistry C.**117,** 6383 (2013).
[3] P. Sen, J. Ghosh, A. Abdullah, P. Kumar, Journal of Chemical Sciences.**115**, 499 (2003).
[4] AR Siekkinen, JM McLellan, J Chen, Y Xia. Chemical physics letter. **432**, 491 (2006).
[5] S Eustis, MA. El-Sayed, Chemical Society Reviews. **35**, 209 (2006).
[6] X Huang, E MA. l-Sayed, Journal of Advanced Research. **1,** 13 (2010).
[7] SK Srivastava, V Arora, S Sapra, BD. Gupta, Plasmonics. **7**, 261 (2012).
[8] KL Kelly, E Coronado, LL Zhao, GC. Schatz, Journal of Physical Chemistry **B107**, 668 (2003).
[9] M Ihara, K Tanaka, K Sakaki, I Honma, K. Yamada, The Journal of Physical Chemistry B. **101**, 5153 (1997).
[10] S-P Ng, X Lu, N Ding, C-ML Wu, C-S Lee, P Solar Energy. **99**, 115 (2014).
[11] N. Chander, A.F. Khan, E. Thouti, S.K. Sardana, Solar Energy.;**109**, 11 (2014).
[12] B. Sebo, N. Huang, Y. Liu, Q. Tai, L. Liang, H. Hu, S. Xu, X.-Z. Zhao, Electrochimica Acta. **112**, 458 (2013)
[13] P Mohan, PS Noonan, MA Nakatsuka, AP Goodwin, Langmuir.;**30**, 12321 (2014).
[14] GA Evtugyn, VB Stepanova, AV Porfireva, AI Zamaleeva, RR. Fakhrullin, Journal of Nanoscience and Nanotechnology. **14**, 6738 (2014).
[15] I Shakir, Z Ali, DJ. Kang, Journal of Alloys and Compounds.; **617**, 707 (2014).
[16] M Cheng, M Zhu, Y Du, P Yang, International Journal of Hydrogen Energy. **38**, 8631 (2013).
[17] T. Sreethawong, S. Yoshikawa, Chemical Engineering Journal. **197**, 272 (2012).
[18] PK Jain, X Huang, IH El-Sayed, MA. El-Sayed, Accounts of Chemical Research. **41**, 1578 (2008).
[19] S Link, MA. El-Sayed, International Reviews in Physical Chemistry. **19**, 409 (2000).
[20] C. Noguez, Journal of Physical Chemistry C. **111**, 3806 (2007).
[21] S. Pillai, K.R. Catchpole, T. Trupke, M.A. Green, Journal of Applied Physics. 2007, 101.
[22] M. Notarianni, K. Vernon, A. Chou, M. Aljada, J. Liu, N. Motta, Solar Energy. **106**, 23 (2014)
[23] CF Bohren, DR. Huffman, Absorption and scattering of light by small particles: John Wiley & Sons; 2008.
[24] J. Becker, Plasmons as sensors: Springer; 2012.
[25] E Thouti, N Chander, V Dutta, VK. Komarala, Journal of Optics 2013, 15.
[26] MD Brown, T Suteewong, RSS Kumar, V D'Innocenzo, A Petrozza, MM Lee, U. Wiesner, H. J. Snaith, Nano Letters. **11,** 438 (2011).
[27] Q Xu, F Liu, Y Liu, K Cui, X Feng, W Zhang, Y Huang, Broadband light absorption enhancement in dye-sensitized solar cells with Au-Ag alloy popcorn nanoparticles. Scientific Reports. 2013;3.
[28] G.K. Darbha, A. Ray, P.C. Ray Acs Nano. **1**, 208 (2007).
[29] S. J. Chen, H.T. Chang Analytical Chemistry **76**, 3727 (2004).

[30] J. R. Lakowicz, Principles of fluorescence spectroscopy. second ed. Kluwer Academic Plenum Press: New York; 1999.
[31] T. Forster, T Discussions of the Faraday Society. **27**, 7 (1959).
[32] M. Procházka, P. Mojzeš, J. Štěpánek, B. Vlčková, P.-Y. Turpin, Analytical Chemistry. **69**, 5103 (1997).
[33] J.-P. Sylvestre, A.V. Kabashin, E. Sacher, M. Meunier, J.H. Luong, Journal of the American Chemical Society. **126**, 7176 (2004).
[34] P. Liu, H. Cui, C. Wang, G. Yang, Physical Chemistry Chemical Physics.;**12**, 3942 (2010).
[35] T. Nakamura, Y. Herbani, D. Ursescu, R. Banici, R.V. Dabu, S. Sato, AIP Advances. **3,** 082101 (2013).
[36] W. Haiss, N.T.K. Thanh, J. Aveyard, D.G. Fernig, Analytical Chemistry. **79**, 4215 (2007).
[37] Tarasenko, N Vladimirovich, A Butsen, E Nevar, N. Savastenko, Applied surface science. **252**, 4439 (2006).
[38] EV Barmina, GA Shafeev, PG Kuzmin, AA Serkov, AV Simakin, NN Melnik. Applied Physics a-Materials Science & Processing.;**115**, 747 (2014).
[39] MK Nazeeruddin, SM Zakeeruddin, R. Humphry-Baker, M Jirousek, P Liska, N Vlachopoulos, V. Shklover, C. H. Fischer, M. Gratzel, Inorganic Chemistry. **38**, 6298 (1999).
[40] MK Nazeeruddin, R Humphry-Baker, P Liska, M. Gratzel, Journal of Physical Chemistry B.**107**, 8981 (2003).
[41] B Oregan, M. Gratzel, Nature.;**353**, 737 (1991).
[42] VV Mokashi, AH Gore, V Sudarsan, MC Rath, SH Han, SR Patil, G. B. Kolekar, Journal of Photochemistry and Photobiology B-Biology. **113**, 63 (2012)
[43] E. Lee, C. Kim, J. Jang, Chemistry-a European Journal.;**19**, 10280 (2013).

* Corresponding author: noriah@utm.my, mohammed.a.alazawi@gmail.com